2023 IEEE International Conference on Robotics and Automation (ICRA 2023)
May 29 - June 2, 2023. London, UK

Atomic-level Tracking and Analyzing of Quantum-dot Motion Steered by an Electrostatic Field Positioned by a Nanorobotic Manipulation Tip *

Zhi Qu, *Student Member, IEEE,* Wenqi Zhang, *Student Member, IEEE,* and Lixin Dong, *Senior Member, IEEE*

Abstract— **Field-control-based nanorobotic manipulation of ions at the single atomic level is an enabling technique for such applications as in-situ prototyping and characterization for fundamental research and rapid product development of nanoscale and quantum devices such as sensors, batteries, neuromorphic devices, and neuro/brain interfaces. Taking the motion of quantum dots (QDs) manipulated by an electrostatic field steered by a probe tip on a target surface as an example, here we show a deep-learning-based approach for their global motion tracking via the individual atoms both on the surface and inside the body. Transmission electron graphs, element analysis, and crystal topology acquired from an aberration-corrected transmission electron microscope (Cs-TEM) are used to identify the positions, types, and structures of the atoms to understand their kinematics. The results show the feasibility of multi-target tracking of homogeneous atoms by their spatial structure projection, which is very encouraging for further extension to the tracking and regulation of crystalline grains, swarms of ions, ion filaments, and single ions.**

I. Introduction

Advanced control of ion migration is a key towards better memories, ion batteries, neuromorphic synapses and neurons, and quantum devices, where motion steering of swarms of ions, crystalline grains, ion filaments, and single ions is involved. Nanorobotic manipulation is enabling a local-field-controlled approach by positioning a probe tip at a proximal site, hence providing a unique and programable way to generate a complex field distribution, which makes near-field ion emission and distribution more controllable in a three-dimensional (3D) space. In field-control-based nanorobotic manipulation, the positioning accuracy of the ions manipulated is not only determined by the localization of the field steered by the manipulation probe, but the repositioning at the target due to the existence of other ions, where self-assembly, crystallization, and phase shifting are typically not avoidable. Understanding and taking the advantage of these phenomenon require real-time visual tracking and servo control at the atomic scale.

The resistive transformation characteristics of the memristor material directly determine the memristor performance. In order to realize stable multi-resistance regulation of memristors, it is necessary to select the memristor functional layer materials and suitable electrode materials with good stability and ease for regulation. The electrochemical metallization mechanism is one of the memristor mechanisms, and the memristor based on this mechanism usually adopts the structure of active electrode/solid electrolyte or dielectric material/inert electrode, in which the active electrode can be oxidized under the voltage applied at both ends [1-7]. The metal cation is generated to migrate to the inert electrode along the electric field direction, and is continuously reduced during the migration process, and the conductive metal wire is generated in the functional layer. The moment the conductive wire is formed, the device transforms from a high resistance state to a low resistance state. When the reverse voltage is applied at both ends of the electrode, the conductive filament can be dissolved or broken, and the device changes from a low-resistance state to a high-resistance state [8-11]. At the same time, the number and shape of conductive wires have a direct impact on the resistance value of the device [12-15]. Controlling the growth number, shape and size of conductive wires is an important basis for the realization of multi-resistance and non-volatile memristor.

After metal atoms are oxidized, the migration of cations in functional layers is usually in form of clusters of QDs. Previous researchers have in-situ characterized and analyzed the growth of conductive filaments from mechanism of electrochemical metallization [8-9], but the migration motion of QDs during the growth of conductive filaments has not been analyzed clearly. The different electrode material and electrode distribution inside, these QDs may migrate in the medium layer and also move on dielectric layer surface. The QDs motion is not only crucial to the study of the memristor mechanism, but also extremely important for the regulation of the growth of conducting filaments.

It is very difficult to analyze the motion of QDs which are migrating inside or on the surface of a material. Firstly, it is hard to identify and track multiple QD targets in the dielectric layer during the in-situ transmission electron microscopy (TEM) characterization[16-22]. Many researchers use manual segmentation and labeling methods, which are extremely laborious and prone to misses [9, 11, 23-25]. The number of QDs is large, and the shapes are similar but slightly different, and the background of in-situ TEM video frame has a variety of noise interference. The dielectric layer introduces streak-like interference to the background in the video frame regardless of the presence of crystal structure of QDs. These bring a great challenge for the robustness of the multi-target detector. Traditional target detection algorithms cannot cope well with such a complex and disordered image environment [25-28]. Therefore, we use a deep learning-based approach to

*This work was partially supported by the National Natural Science Foundation of China (grant no. 62127810) and the General Research Fund of Hong Kong (Project nos. 11219419, 11213720, and 11217221).

All authors are with Department of Biomedical Engineering, City University of Hong Kong, Hong Kong 999077, China (email: QU.Zhi@my.cityu.edu.hk; wqzhang22-c@my.cityu.edu.hk; corresponding author to provide phone: +852-3442-9545; email: l.x.dong@cityu.edu.hk).

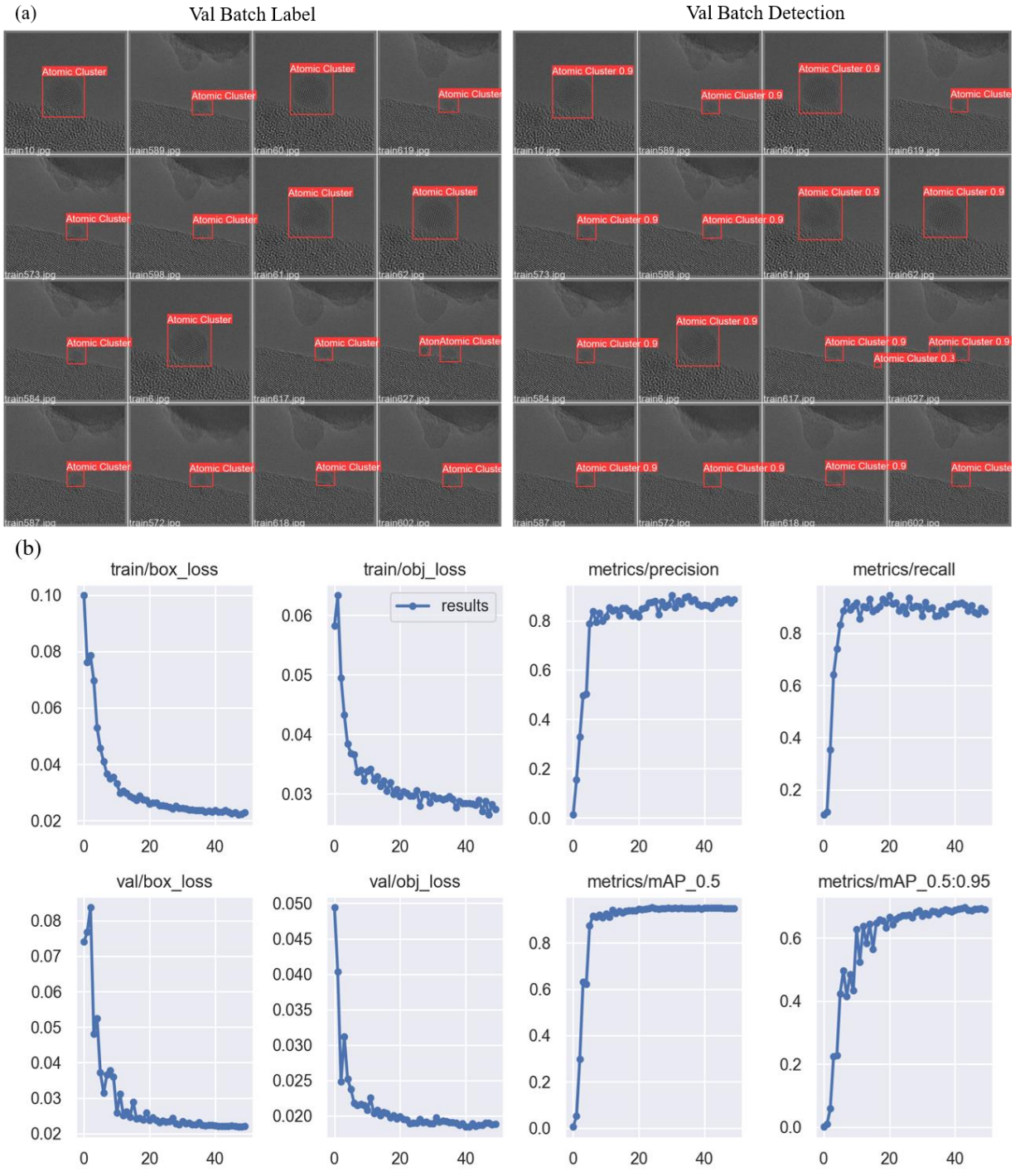

Figure 1. Neural network training results. (a) Comparison of validation dataset labels and detection results during training. (b) YOLOv5 network training results graph.

build a TEM QD migration motion dataset and train the YOLOv5 neural network to detect the multi-QD targets [29]. The DeepSORT algorithm is used to correlate each detected object in the before and after video frames to complete the detection of QDs and obtain the location of the object [30].

However, when QDs migrate inside the material or move on the surface interface, they also rotate around the center of mass, which brings great difficulty to the motion analysis. In order to obtain the rotation of QDs, the crystal structure of QD in each in-situ TEM video frame was analyzed with fast Fourier transform, and the spatial rotation of QDs was indirectly obtained. The discrete centroid position and rotation attitude are obtained by tracking and crystal analysis, and the spatial attitude interpolation is performed to obtain the trajectory curve of the target QDs. The velocity curve and acceleration curve are obtained by further differentiating the trajectory. At the same time, since the distribution of QDs in space is basically symmetrical, the number of atoms in the QDs can be estimated, and the force can be estimated by combining the acceleration.

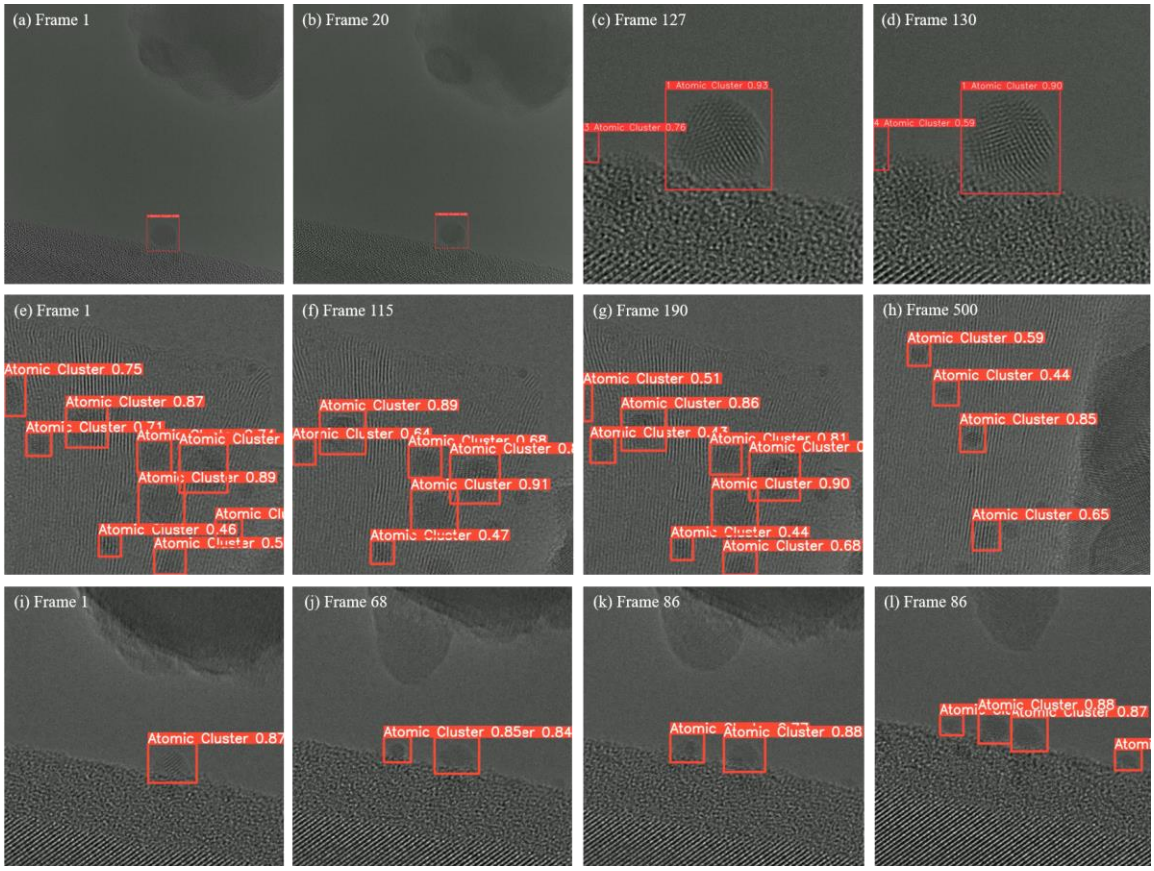

Figure 2. Multi-target detection and tracking for in-situ TEM characterization by YOLOv5 + DeepSORT

II. Multi-target Tracking of QD Based on Neural Network

The growth of conductive filaments is the basis of the resistive characteristics of memristors, and the characterization and regulation of the QDs that make up the conductive filaments during the growth process is the focus of attention. Therefore, the accurate tracking of QDs motion in the dielectric layer is crucial. Whether it is single-target tracking or multi-target tracking, the core is the detection of the target, and the detector directly determines the tracking accuracy. Target tracking first gives the original frame, then runs the target detector to obtain the boundary and position information of the target. Then it calculates the features of the detected objects, usually visual features and motion features, and then calculates the probability that the objects detected in the two frames before and after belong to the same target, and determines whether the objects in different frames are the same.

Transmission electron microscopy (TEM) was used to characterize the migration of QDs inside and on the surface of the material in situ and obtain the video frame of the target. Transmission electron microscope after the electron beam and accelerate convergence projected onto a very thin dielectric layer zone, electronic and atomic collisions in the samples and changed direction, produce solid angle scattering, due to the different physical properties of the sample area of the electrical signals generated by collision types, scattering angle, energy and other characteristics are different. Therefore, different contrast degrees are formed when imaging on the photosensitive element. Due to the special imaging principle and working environment of transmission electron microscope, when QDs are used as the detection target, the dielectric layer is the base, and there will be a lot of noise points in the imaging results. And dielectric layer may be a crystal or amorphous materials, and orderly lattice fringe or disorderly chaotic amorphous stripes, the presence of these stripes for quantum interference detection is very large, and the QDs and the contrast of the base were similar [31]. Therefore, the key of the problem is to establish a detector that can automatically detect the QDs accurately and quickly from the complex background.

YOLOv5 is an efficient and stable deep learning based detector neural network [29], which is trained supervised by building a QD migration motion dataset which are derived from three different scenes. The electrodes are arranged in lateral structure, and there is also a combination structure of fixed and mobile electrodes. The active electrode materials are Ag and Li. The functional layer is a dielectric material with crystal structure, using SiO_2 and Si_3N_4. Some key frames are randomly extracted from the in-situ characterization videos of three scenes, a total of 814 key frame images. In order to improve the training efficiency and shorten the training time, the original TEM video is cropped to 640×640pixel, and the QDs in the images are labeled for neural network training, of which 585 images are divided into training sets. The training framework of the neural network is Pytorch, and to prevent overfitting due to the relatively small sample size, setting epoch=50, batch size=8, and a total of 3700 iterations [32]. The comparison between the labeling results and the detection results of the verification dataset in the training process is shown in Figure 1(a). It can be seen that the QDs detected in

the verification dataset image correspond to the labeled label one by one with high confidence. The training result of the network is shown in Figure 1(b), which has a well training effect.

DeepSORT and YOLO neural network were used to track the migration motion of QDs. Firstly, we use YOLO detector to get the location of QDs (generating Detections). DeepSORT will use Kalman filter to predict the tracks of the next frame according to the target location of this frame. Then, the Hungarian algorithm is used to match the predicted tracks with the detections obtained by the detector of the next frame (cascade matching and IOU matching), so as to complete the correspondence between the targets of the previous and subsequent frames [30]. The above process can be repeated to track the QDs. The migration motion of QDs in different scenes is analyzed. It can be seen from Figure 2 that in the process of QDs moving on the surface of the substrate, the position of QDs in every frame can be accurately identified. Even when new QDs appear in the scene, the target can be detected and tracked in time.

The multi-target tracking method of YOLOv5 combined with DeepSORT can efficiently and accurately recognize and track the migrating and moving QDs in the memristor functional layer. This method provides a means of detecting and tracking the growth mechanism and regulation of conductive filaments in memristor. It basically replaces manual labeling and significantly improves the tracking accuracy.

III. Posture and Motion Analysis of QDs Based on In-situ Crystal Orientation Change

The migration of QDs in the material or the movement on the surface of the material is a composite of translation and rotation. The position change caused by the translational motion on the projection plane is determined by the target tracking algorithm, but the posture change caused by the rotation of QDs cannot be determined only by the high-resolution characterization of transmission electron microscopy. The in-situ characterization of transmission electron microscopy can obtain a variety of information of the sample. Through phase analysis of QDs, the crystal structure and crystal direction of QDs can be determined. The change of crystal direction can clearly reflect the rotational motion of QDs. Therefore, after determining the composition and crystal structure of the QD material, the change of crystal direction can be analyzed to determine the pose in each frame. By interpolating the discrete posture points, the approximate rotational posture trajectory of the QDs can be obtained.

The Ag nanoprobe was used as the active electrode and SiO_2 was used as the functional layer material to characterize and analyze the motion of Ag QDs on the functional layer surface under the action of electric field. Fast Fourier transform was performed on each frame of the TEM in situ high-resolution characterization map of the QD region to obtain the diffraction map of the QD region, and according to the distribution and position of the diffraction spots in the map,

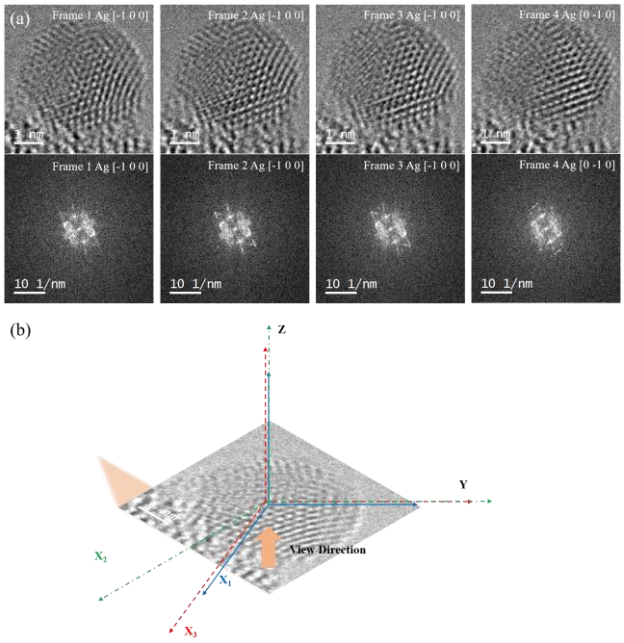

Figure 3. QD crystal analysis. (a) Diffraction and crystal orientation analysis of QD crystals. (b) Establishing coordinate system in analysis of QD motion. ($X_1Y_1Z_1$ is TEM coordinate system, $X_2Y_2Z_2$ is the crystal structure coordinate system, and $X_3Y_3Z_3$ is the Cartesian coordinate system solidly connected to the crystal)

the crystal structure and crystal orientation of the QD could be determined in combination with the type of material, as shown in Figure 3(a).

In order to accurately describe the rotational motion of the crystal, an appropriate reference coordinate is established according to the crystal structure and the position of the QDs in the initial frame. There are three coordinate systems: (1) Fixed coordinate system: fixed with transmission electron microscope, Cartesian coordinate system. (2) Crystal structure coordinate system: solid connected with the crystal, its coordinate axes are not necessarily orthogonal, related to its crystal structure. (3) The relative coordinate system on the crystal, which is connected to the crystal and remains relatively stationary with the coordinate system of the crystal structure, Cartesian coordinate system, which is used to establish the relationship between the first two coordinate systems in the rotation. In the initial frame, the relative positions of the three coordinates and their relationship with the imaging perspective are shown in Figure 3(b).

After analyzing the crystalline phase of the QD, the material and structure can be identified, and the relative relationship between the axes of the crystal structure coordinate can be determined. Combined with the crystal orientation of the current frame, the angle of rotation of the crystal structure coordinate system with respect to the electron microscope coordinate system can be obtained for the current frame. Thus, the rotation matrix $\boldsymbol{R}$ of a QD rotated by $\delta\theta$ about the axis $\boldsymbol{k}$ past the origin of TEM coordinate can be expressed as (1):

$$\boldsymbol{R}(\boldsymbol{k},\delta\theta)=\begin{bmatrix} k_xk_x(1-\cos\theta)+\cos\theta & k_yk_x(1-\cos\theta)-k_z\sin\theta & k_zk_x(1-\cos\theta)+k_y\sin\theta \\ k_xk_y(1-\cos\theta)+k_z\sin\theta & k_yk_y(1-\cos\theta)+\cos\theta & k_zk_y(1-\cos\theta)-k_x\sin\theta \\ k_xk_z(1-\cos\theta)-k_y\sin\theta & k_yk_z(1-\cos\theta)+k_x\sin\theta & k_zk_z(1-\cos\theta)+\cos\theta \end{bmatrix} \quad (1)$$

The crystal phase analysis of the QD region for each frame is performed to obtain the rotation matrix of the QD about the transmission electron microscope coordinate system at each discrete moment, and to determine the positional matrix of the QD for each frame. In order to further analyze the motion state of the QDs and the subsequent regulation of the conductive filament growth, it is necessary to estimate the successive positional trajectories of the QDs. In this paper, the discrete poses of QDs are interpolated using quaternion spherical cubic interpolation to obtain the absolute motion pose trajectories [33]. The quaternion spherical cubic interpolation is different from the general spherical linear interpolation, and the trajectories obtained by this interpolation method are segmented cubic Bessel curves, and the trajectories are not only smooth and continuous, but also differentiable in the first order. Moreover, this interpolation method can guarantee the shortest spatial rotation distance of quantum points. Analyzing the shape center positions of the four QDs in Figure 3(a), the motion of the QDs in these frames of time is pure rolling, and then quaternion spherical cubic interpolation is performed on the discrete pose, and the continuous rotation space pose is obtained as shown in Figure 4 (the coordinate axes have been normalized).

The change of the centroid position of the QD represents the information of its plane motion, which can be obtained by target tracking, and then the trajectory of the centroid motion can be obtained by interpolating the discrete position points. Here, we focus on the analysis of the rotational trajectory of QDs, and estimate the angular velocity and angular acceleration of QDs using the continuous trajectory points obtained by interpolation.

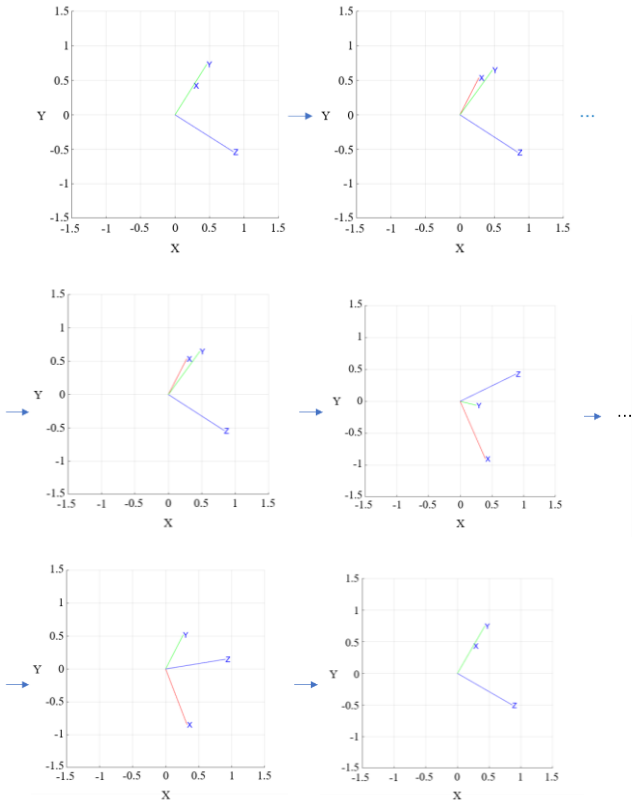

Figure 4. QD pose trajectories at certain moments based on quaternion spherical cubic interpolation

$$\begin{cases} \Delta\theta = \boldsymbol{p} \otimes \boldsymbol{q} = \begin{bmatrix} p_w q_w - p_v' q_v \\ p_w q_v + q_w p_v + p_v \times q_v \end{bmatrix} \\ \omega = \dfrac{\Delta\theta}{\Delta t} \end{cases} \tag{2}$$

According to (2), the angular velocity is calculated by using the quadratic ($\boldsymbol{p}$, $\boldsymbol{q}$) angle of the adjacent points after interpolation, and the tangential acceleration is calculated by making the difference between the angular velocity and the tangential acceleration. The calculated curves of the angular velocity and tangential acceleration of the quantum point with time are shown in Figure 5.

Using high-resolution TEM images and diffraction patterns of QDs, the spatial rotational posture of QDs can be accurately obtained. This method provides a new research tool for studying the motion of nanoscale crystal structures and a new idea for the calculation of molecular kinematics and dynamics characteristics based on in situ experimental characterization and analysis. It provides a research basis for the modulation of nanoclusters or QDs.

IV. Conclusion

The neural network-based multi-QD detection and tracking method improves the accuracy and efficiency of identifying and tracking nanoclusters and QDs in a TEM for in situ characterization, and provides a new auxiliary means for in-depth study of the migration and surface motion of QDs inside the memristor material, improves the automation of QD motion information extraction, and provides a great convenience for studying the mechanism of electrochemical metallization based on conductive fine wires. The combination of multiple sensing information in the TEM in situ process has been utilized to perform crystal phase analysis of the QD crystal structure, which enables the

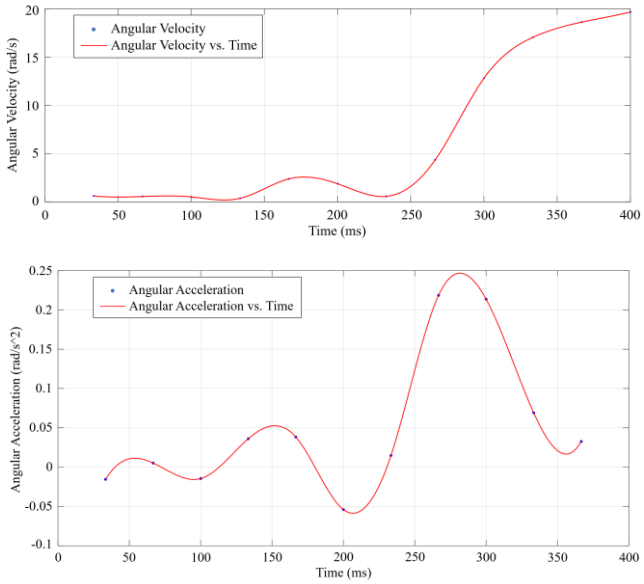

Figure 5. Curves of the angular velocity magnitude and tangential acceleration magnitude of ODs over time

capture of the spatial rotation posture of QDs. From the perspective of multiple in situ sensing combined with computation, it provides not only a new method for the motion analysis of nanoscale crystal structures but a research basis for nanostructure growth regulation. The results have shown the feasibility of multi-target tracking of homogeneous atoms by their spatial structure projection during field-control-based nanorobotic manipulation, which is very encouraging for further extension to the tracking and regulation of crystalline grains, swarms of ions, ion filaments, and single ions; enabling technique for such applications as in-situ prototyping and characterization for fundamental research and rapid product development of nanoscale and quantum devices such as sensors, batteries, neuromorphic devices, and neuro/brain interfaces.

REFERENCES

[1] F. Alibart, E. Zamanidoost, and D. B. Strukov, "Pattern classification by memristive crossbar circuits using ex situ and in situ training," *Nature Communications,* vol. 4, art. no. 2072, Jun 2013.

[2] J. J. S. Yang, D. B. Strukov, and D. R. Stewart, "Memristive devices for computing," *Nature Nanotechnology,* vol. 8, no. 1, pp. 13-24, Jan 2013.

[3] M. Prezioso, F. Merrikh-Bayat, B. D. Hoskins, G. C. Adam, K. K. Likharev, and D. B. Strukov, "Training andoperation of an integrated neuromorphic network based on metal-oxide memristors," *Nature,* vol. 521, no. 7550, pp. 61-64, May 2015.

[4] E. J. Fuller, F. El Gabaly, F. Leonard, S. Agarwal, S. J. Plimpton, R. B. Jacobs-Gedrim, C. D. James, M. J. Marinella, and A. A. Talin, "Li-ion synaptic transistor for low power analog computing," *Advanced Materials,* vol. 29, no. 4, art. no. 1604310, Jan 2017.

[5] X. J. Zhu, Q. W. Wang, and W. D. Lu, "Memristor networks for real-time neural activity analysis," *Nature Communications,* vol. 11, no. 1, art. no. 2439, May 2020.

[6] Z. Fan, X. D. Fan, A. Li, and L. X. Dong, "In situ forming, characterization, and transduction of nanowire memristors," *Nanoscale,* vol. 5, no. 24, pp. 12310-12315, 2013.

[7] C. Nyenke and L. X. Dong, "Fabrication of a w/cuxo/cu memristor with sub-micron holes for passive sensing of oxygen," *Microelectronic Engineering,* vol. 164, pp. 48-52, Oct 2016.

[8] S. J. Choi, G. S. Park, K. H. Kim, S. Cho, W. Y. Yang, X. S. Li, J. H. Moon, K. J. Lee, and K. Kim, "In situ observation of voltage-induced multilevel resistive switching in solid electrolyte memory," *Advanced Materials,* vol. 23, no. 29, pp. 3272-3277, Aug 2011.

[9] J. Y. Chen, C. L. Hsin, C. W. Huang, C. H. Chiu, Y. T. Huang, S. J. Lin, W. W. Wu, and L. J. Chen, "Dynamic evolution of conducting nanofilament in resistive switching memories," *Nano Letters,* vol. 13, no. 8, pp. 3671-3677, Aug 2013.

[10] W. A. Hubbard, A. Kerelsky, G. Jasmin, E. R. White, J. Lodico, M. Mecklenburg, and B. C. Regan, "Nanofilament formation and regeneration during Cu/Al_2O_3 resistive memory switching," *Nano Letters,* vol. 15, no. 6, pp. 3983-3987, Jun 2015.

[11] Y. C. Yang, P. Gao, S. Gaba, T. Chang, X. Q. Pan, and W. Lu, "Observation of conducting filament growth in nanoscale resistive memories," *Nature Communications,* vol. 3, art. no. 732, Mar 2012.

[12] D. H. Kwon, K. M. Kim, J. H. Jang, J. M. Jeon, M. H. Lee, G. H. Kim, X. S. Li, G. S. Park, B. Lee, S. Han, M. Kim, and C. S. Hwang, "Atomic structure of conducting nanofilaments in TiO_2 resistive switching memory," *Nature Nanotechnology,* vol. 5, no. 2, pp. 148-153, Feb 2010.

[13] T. Fujii, M. Arita, Y. Takahashi, and I. Fujiwara, "In situ transmission electron microscopy analysis of conductive filament during solid electrolyte resistance switching," *Applied Physics Letters,* vol. 98, no. 21, art. no. 212104, May 2011.

[14] K. Terabe, T. Tsuchiya, and T. Tsuruoka, "A variety of functional devices realized by ionic nanoarchitectonics, complementing electronics components," *Advanced Electronic Materials,* vol. 8, no. 8, p. 17, art. no. 2100645, Aug 2022.

[15] H. T. Zhang, T. J. Park, A. Islam, D. S. J. Tran, S. Manna, Q. Wang, S. Mondal, H. M. Yu, S. Banik, S. B. Cheng, H. Zhou, S. Gamage, S. Mahapatra, Y. M. Zhu, Y. Abate, N. Jiang, S. Sankaranarayanan, A. Sengupta, C. Teuscher, and S. Ramanathan, "Reconfigurable perovskite nickelate electronics for artificial intelligence," *Science,* vol. 375, no. 6580, pp. 533-539, Feb 2022.

[16] L. X. Dong, X. Y. Tao, L. Zhang, X. B. Zhang, and B. J. Nelson, "Nanorobotic spot welding: Controlled metal deposition with attogram precision from copper-filled carbon nanotubes," *Nano Letters,* vol. 7, no. 1, pp. 58-63, Jan. 2007.

[17] M. Nakajima, F. Arai, L. X. Dong, and T. Fukuda, "A hybrid nanorobotic manipulation system integrated with nanorobotic manipulators inside scanning and transmission electron microscopes," in *Proc. of 2004 4th IEEE Conf. on Nanotechnology (IEEE-NANO2004)*, Munich, Germany, 2004, pp. 462-464.

[18] M. J. Zhang, S. Lenaghan, L. J. Xia, L. X. Dong, W. He, W. Henson, and X. D. Fan, "Nanofibers and nanoparticles from the insect-capturing adhesive of the sundew (drosera) for cell attachment," *Journal of Nanobiotechnology,* vol. 8, no. 8, Aug. 2010.

[19] Z. Fan, X. Y. Tao, X. D. Cui, X. D. Fan, X. B. Zhang, and L. X. Dong, "Metal-filled carbon nanotube based optical nanoantennas: Bubbling, reshaping, and in situ characterization," *Nanoscale,* vol. 4, no. 18, pp. 5673-5679, Sep 21 2012.

[20] C. H. Sun, W. K. Dong, L. Yang, X. T. Zuo, L. X. Bao, Z. Hua, X. X. Chang, R. Cai, H. S. Chen, X. D. Han, Y. He, T. S. Liu, R. W. Shao, and L. X. Dong, "Anisotropic lithium-ion migration and electro-chemo-mechanical coupling in sb2se3 single crystals," *Science China-Materials,* vol. 65, no. 10, pp. 2657-2664, Oct 2022.

[21] R. Cai, W. Q. Zhang, J. H. Zhou, K. S. Yang, L. F. Sun, L. Yang, L. G. Ran, R. W. Shao, T. Fukuda, G. Q. Tan, H. D. Liu, J. Y. Wan, Q. B. Zhang, and L. X. Dong, "Unraveling atomic-scale origins of selective ionic transport pathways and sodium-ion storage mechanism in bi2s3 anodes," *Small Methods,* vol. 6, no. 11, art. no. 2200995, Nov 2022.

[22] R. Cai, L. X. Bao, W. Q. Zhang, W. W. Xia, C. H. Sun, W. K. Dong, X. X. Chang, Z. Hua, R. W. Shao, T. Fukuda, Z. F. Sun, H. D. Liu, Q. B. Zhang, F. Xu, and L. X. Dong, "In situ atomic-scale observation of size-dependent (de) potassiation and reversible phase transformation in tetragonal fese anodes," *Infomat,* vol. 5, no. 1, art. no. e12364, Jan 2023.

[23] Y. Hou, U. Celano, L. Goux, L. Liu, A. Fantini, R. Degraeve, A. Youssef, Z. Xu, Y. Cheng, J. Kang, M. Jurczak, and W. Vandervorst, "Sub-10 nm low current resistive switching behavior in hafnium oxide stack," *Applied Physics Letters,* vol. 108, no. 12, art. no. 123106, Mar 2016.

[24] X. J. Zhu, D. Li, X. G. Liang, and W. D. Lu, "Ionic modulation and ionic coupling effects in MoS_2 devices for neuromorphic computing," *Nature Materials,* vol. 18, no. 2, pp. 141-148, Feb 2019.

[25] G. Tesauro, "Temporal difference learning and td-gammon," *Communications of the Acm,* vol. 38, no. 3, pp. 58-68, Mar 1995.

[26] B. K. P. Horn and B. G. Schunck, "Determining optical-flow," *Artificial Intelligence,* vol. 17, no. 1-3, pp. 185-203, 1981.

[27] M. Piccardi, "Background subtraction techniques: A review," in *IEEE International Conference on Systems, Man and Cybernetics*, The Hague, Netherlands, 2004, pp. 3099-3104.

[28] R. Brunelli, *Template matching techniques in computer vision: Theory and practice*: Wiley, 2009.

[29] A. Bochkovskiy, C. Y. Wang, and H. Y. M. Liao, "Yolov4: Optimal speed and accuracy of object detection," *arXiv preprint,* art. no. arXiv:2004.10934, 2020.

[30] N. Wojke, A. Bewley, and D. Paulus, "Simple online and realtime tracking with a deep association metric," in *24th IEEE International Conference on Image Processing (ICIP)*, Beijing, P. R. China, 2017, pp. 3645-3649.

[31] L. Reimer, *Transmission electron microscopy: Physics of image formation and microanalysis* vol. 36: Springer, 2013.

[32] N. Srivastava, G. Hinton, A. Krizhevsky, I. Sutskever, and R. Salakhutdinov, "Dropout: A simple way to prevent neural networks from overfitting," *Journal of Machine Learning Research,* vol. 15, pp. 1929-1958, Jun 2014.

[33] E. B. Dam, M. Koch, and M. Lillholm, *Quaternions, interpolation and animation* vol. 2: Copenhagen: Datalogisk Institut, Københavns Universitet, 1998.